RSC Advances

ROYAL SOCIETY
OF CHEMISTRY

www.rsc.org/advances

Journal Name

ARTICLE TYPE

Binding of an anionic fluorescent probe with calf thymus DNA and effect of salt on the probe-DNA binding: A spectroscopic and molecular docking investigation

Saptarshi Ghosh[a], Pronab Kundu[a], Bijan Kumar Paul[b], and Nitin Chattopadhyay[a],*

Binding interaction of a biologically relevant anionic probe molecule, 8-anilino-1-naphthalene sulfonate (ANS) with calf-thymus deoxyribonucleic acid (ctDNA) has been investigated exploiting vivid spectroscopic techniques together with molecular docking study. Significant modifications in the
10 absorption and emission profiles, the determined binding constant, micropolarity analysis, circular dichroism (CD) spectral study, comparative binding study with ethidium bromide (EtBr) — an intercalative binder, thermometric experiment relating to the helix melting of ctDNA and blind molecular docking simulation confirm the groove binding of ANS with ctDNA. Furthermore, a remarkable enhancement is observed in the fluorescence intensity as well as in the fluorescence lifetime of the DNA-
15 bound probe with the addition of salts. Reduction in the electrostatic repulsion between the ANS and DNA at high salt concentration has been assigned responsible for this observation. Besides providing an insight into the probe-DNA interaction, the work implies that the binding interaction of a negatively charged probe with DNA can be enhanced considerably by the addition of salts.

Introduction

20 Deoxyribonucleic acid (DNA) is perhaps the most studied biopolymer because of its importance in controlling the heredity of life by its base sequence. DNA is involved in many biologically imperative phenomena like gene transcription,[1] mutagenesis,[2] gene expression,[3,4] etc. and thus legitimately
25 depicted as one of the nature's most elementary conduits for developing and functioning of living organisms.[3] In recent times, binding of small molecules with DNA and revelation of structural aspects of such bindings come out to be an emerging topic of interest from the perspective of medicinal or clinical research.[5,6]
30 These studies have colossal significance and application in various important biological processes including cancer chemotherapy for the designing and development of new and more efficient therapeutic agents targeted to DNA. Literature suggests that several electronic and structural factors dictate the
35 binding affinity as well as the sequence specificity of small molecules towards the DNA.[7,8] Small molecules bind to the DNA double helix principally by three dominant modes referred to as (i) intercalative binding where the molecule intercalates within the base pairs of nucleic acid, (ii) groove binding involving
40 hydrogen bonding or van der Waal's interaction in the deep major groove or the shallow minor groove of the DNA helix and (iii) electrostatic binding between the negatively charged DNA phosphate backbone and cationic or positive end of the molecules.[9,10]
45 There are lots of reports available in the literature comprising

of interaction of neutral and positively charged probes with DNA.[3,6-8,10-12] However, there are only few scattered studies[13,14] done so far with negatively charged molecular probes. In the present article, we have made a successful endeavour to
50 demonstrate the binding interaction of an anionic fluorophore, 8-anilino-1-naphthalene sulfonate (ANS) (Scheme 1) with calf-thymus DNA (ctDNA). ANS is known to be an excellent molecular probe as polarity sensor for organized and aggregated systems like micelles, proteins, lipid bilayer membranes,
55 polymeric gel etc.[15-21] Schonbrunn and co-workers have studied the interaction of ANS with an antibiotic target and essential enzyme for bacterial cell wall biosynthesis.[22] In a recent work from our lab, ANS was shown to be electrostatically pushed inside the micellar interior by the halide ions.[23] In the present
60 work, we have investigated the mode of interaction of this biologically significant probe, ANS with the most relevant biomacromolecule, DNA, through several spectroscopic techniques. The steady-state and time-resolved fluorometric experiments, comparative binding study with the well-known
65 DNA intercalator ethidium bromide (EtBr), circular dichroism spectral study and DNA helix melting experiment unambiguously establish that ANS binds with ctDNA through groove binding fashion. Blind molecular docking simulation corroborates the experimental findings in a nice way depicting the groove binding
70 of the probe with DNA.

Apart from the successful unveiling of groove binding mode of ANS with ctDNA, we have investigated the salt effect on the probe-DNA interaction. Steady state and time resolved fluorometric responses of the probe in the DNA environment in

the presence of added salts reveal that the binding between the probe and DNA is favoured by the increased ionic strength. Reduction in the electrostatic repulsion between the probe and the DNA backbone due to the increased ionic strength of the solution has been assigned responsible for this favourable probe-DNA interaction. As expected, the effect is found to be enhanced in the presence of ions of higher valence.
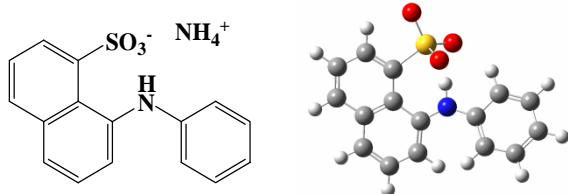
Scheme 1. Schematic and optimized structures of ANS.

Experimental

Materials

8-anilino-1-naphthalene sulfonate (ANS) was purchased from Sigma-Aldrich (USA) and used as received without further purification. Ethidium bromide (EtBr) and ctDNA (Molecular wt. 8.4 MDa) obtained from Sisco Research Laboratories (SRL), India; N-[2-hydroxyethyl]piperazine-N-[2-ethanesulphonic acid] (HEPES) buffer, sodium chloride (NaCl), sodium bromide (NaBr), sodium iodide (NaI), sodium sulfate (Na_2SO_4) and sodium phosphate (Na_3PO_4) procured from Sigma-Aldrich (USA), spectroscopic grade 1,4-dioxane (Spectrochem, India) and methanol (Merck, India) were used as received. Deionised water from a Milli-Q water purification system (Millipore) was used throughout the experiment. All the experiments were performed using HEPES buffer of 0.01 M (pH = 7).

Stock solution of ctDNA was prepared by dissolving solid ctDNA in HEPES buffer (pH = 7) and stored at 4 °C. The purity of ctDNA was verified by monitoring the ratio of absorbance at 260 nm to that at 280 nm, which was in the range 1.8—1.9. The concentration of ctDNA solution was determined spectrophotometrically using ε_{DNA} = 6,600 mol^{-1} dm^3 cm^{-1} at 258 nm.[24] The concentration of ANS was kept at 10 μM throughout the study unless otherwise specified. Freshly prepared solutions were used for all the measurements.

Steady state spectral measurements

Shimadzu UV-2450 absorption spectrophotometer (Shimadzu Corporation, Kyoto, Japan) was used for the steady state absorption studies. Steady state fluorescence and fluorescence anisotropy measurements were carried out in a Horiba Jobin Yvon Fluoromax-4 spectrofluorometer. Fluorescence anisotropy (r) is defined as

$$r = (I_{VV} - G \cdot I_{VH}) / (I_{VV} + 2G \cdot I_{VH}) \qquad (1)$$

where I_{VV} and I_{VH} are the emission intensities obtained with the excitation polarizer oriented vertically and emission polarizer oriented vertically and horizontally, respectively. The G factor is defined as[25]

$$G = I_{HV} / I_{HH} \qquad (2)$$

where the intensities I_{HV} and I_{HH} refer to the vertical and horizontal positions of the emission polarizer, with the excitation polarizer being horizontal. The experiments were carried out at an ambient temperature of 298 K.

Time resolved fluorescence decay measurements

Time resolved fluorescence decay measurements were done by the time-correlated single photon counting (TCSPC) technique in Horiba–Jobin–Yvon FluoroCube fluorescence lifetime system using NanoLED at 370 nm (IBH, UK) as the excitation source and TBX photon detection module as the detector. The decays were analyzed using IBH DAS-6 decay analysis software. The lamp profile was collected by placing a scatterer (dilute micellar solution of sodium dodecyl sulfate in water) in place of the sample. Goodness of fits was evaluated from χ^2 criterion and visual inspection of the residuals of the fitted function to the data. Mean (average) fluorescence lifetimes (τ_{avg}) for triexponential iterative fittings were calculated from the decay times (τ_1, τ_2 and τ_3) and the pre-exponential factors (a_1, a_2 and a_3) using the following relation

$$\tau_{avg} = a_1\tau_1 + a_2\tau_2 + a_3\tau_3 \qquad (3)$$

Circular dichroism spectroscopy

Circular dichroism (CD) spectra were recorded on a JASCO J-815 spectropolarimeter (Jasco International Co., Hachioji, Japan) using a rectangular quartz cuvette of path length 1 cm. The CD profiles were obtained employing a scan speed of 50 nm/min and appropriate baseline corrections were made by using aqueous buffer solution. The experiments were performed at room temperature (298 K) with air-equilibrated solutions. Concentrations of ctDNA and probe are mentioned in the relevant figure.

Helix melting experiment

For DNA helix melting experiment, the pre-fixed temperatures were set using a high precession peltier (Wavelength Electronics, USA, Model No. LFI-3751, temperature stability within 0.002 ^{0}C) that was attached to the aforesaid spectrophotometer. Adequate time was provided before each measurement for attainment of the temperature throughout the solution inside the cuvette.

Molecular docking study

For molecular docking simulation, the native structure of DNA was taken from the Protein Data Bank having PDB ID: 1BNA (B-DNA).[26] Docking studies were performed with AutoDock 4.2 suite of programs that utilizes the Lamarckian Genetic Algorithm (LGA) implemented therein. For docking of ANS with DNA, the required file for the ligand (ANS) was created through combined use of Gaussian 03W[27] and AutoDock 4.2[28] software packages. The geometry of ANS was first optimized at DFT//B3LYP/6-31G (d,p) level of theory using Gaussian 03W suite of programs and the resultant geometry was read in AutoDock 4.2 software in compatible file format, from which the required file was generated in AutoDock 4.2. The grid size was set to 40, 40, and 100 along X-, Y-, and Z-axis with 0.375 Å grid spacing. The AutoDocking parameters used were as follows: GA population size = 150; maximum number of energy evaluations = 250000; GA crossover mode = two points. The lowest binding energy conformer was searched out of 10 different conformations for

each docking simulation and the resultant minimum energy conformation was applied for further analysis. The PyMOL software package was used for visualization of the docked conformations.[29]

Results and discussion

Steady state absorption and emission study

The UV-Vis absorption spectrum of ANS (10 μM) in aqueous buffer solution shows a low energy broad band with λ_{abs}^{max} at ~360 nm[20] as shown in Fig. 1. Addition of ctDNA to the buffered solution of ANS causes considerable decrease in the absorbance without any shift in λ_{abs}^{max}. The appreciable lowering in absorbance in the presence of DNA implies a binding interaction between the two. However, absence of any shift in λ_{abs}^{max} rules out the possibility of intercalative binding since this mode of binding of small molecules with DNA usually causes a large shift in the absorption maxima.[10] Consistent with the literature revealing that groove binding results in an insignificant (or small) shift in the absorption spectra,[2,7,11,13] the observation is ascribed to groove binding.
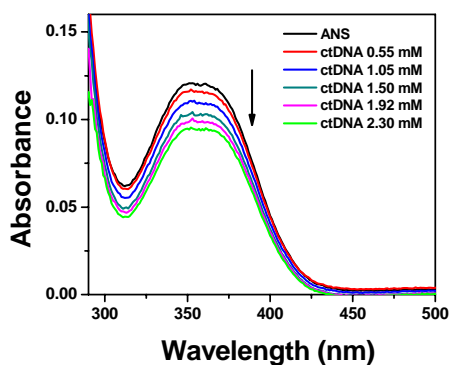
Fig. 1 Absorption spectra of ANS in aqueous buffer and in the presence of different ctDNA concentrations. Concentrations of ctDNA are labeled in the legends. [ANS] = 10 μM.

Emission spectrum of ANS in HEPES buffer shows a single and unstructured band peaking at around 520 nm upon excitation at 370 nm.[20,23] Gradual addition of ctDNA to the buffered solution of ANS leads to an appreciable increase in the emission intensity along with a considerable hypsochromic shift of ~12 nm. Fig. 2 shows the variation in the fluorescence spectra of ANS in the presence of added ctDNA. To obtain a clearer picture of probe-DNA interaction, we have plotted the variation of the fluorescence intensity and the emission maximum of ANS against ctDNA concentration in Fig. 3 (a). The figure reveals that with an increase in the DNA concentration the emission intensity of ANS increases, eventually attaining a plateau. The maximum of the ANS emission band also shows a gradual blue shift and then remains unaffected after a certain DNA concentration. The change in the fluorometric response (both increase in the intensity and the blue shift of the emission maximum) indicates binding of the probe with the ctDNA. The appreciable blue shift in the emission maximum of the ANS in DNA environment suggests that the probe is experiencing a less polar environment than the aqueous buffer milieu. The emission characteristics of ANS in ctDNA environment is in agreement with the behaviour of the

probe in less polar media.[20,23] It is pertinent to mention here that the width of the emission spectrum (fwhm) of DNA bound probe is larger than that of aqueous buffer. The larger fwhm of ANS in ctDNA environment may be ascribed to the multiple locations of the probe and the heterogeneity of the microenvironment.[30]
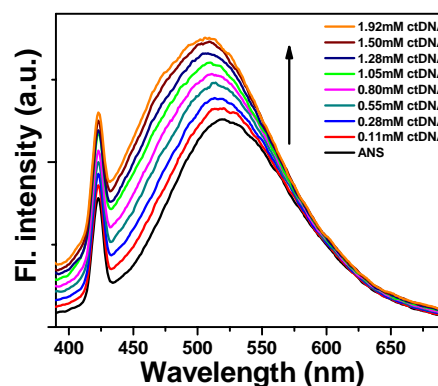
Fig. 2 Emission spectra of ANS in presence of different concentrations of ctDNA. The concentrations of the ctDNA solutions are labeled in the legends. The sharp peak around 423 nm arises due to the Raman scattering. λ_{exc} = 370 nm, [ANS] = 10 μM.

Since the binding constant value gives an idea about the strength of binding between the probe and the macromolecule, we have exploited both the absorption and fluorescence titration data to determine the binding constant using the modified Benesi-Hildebrand equation[31] as given below.[31,32-34]

$$\frac{1}{\Delta F} = \frac{1}{\Delta F_{max}} + \frac{1}{K \Delta F_{max}} \frac{1}{[L]}$$

where $\Delta F = F_x - F_0$ and $\Delta F_{max} = F_\infty - F_0$ where F_0, F_x and F_∞ are the absorbance or fluorescence intensities of ANS in the absence of ctDNA, at an intermediate ctDNA concentration, and at a concentration for complete interaction respectively; K is the binding constant and [L] is the ctDNA concentration. Plot of $1/\Delta F$ against [ctDNA]$^{-1}$ (Fig. 3 (b)) from fluorescence measurements gives a straight line (R=0.996) indicating one-to-one interaction between the probe and the ctDNA. The binding constant (K) is determined from the ratio of the intercept to slope of the plot and for the present system the determined value comes out to be 534 M^{-1} at the experimental temperature (298 K). The corresponding linear plot (R=0.996) using the absorption data, given in the ESI (Fig. S1), yields a value of 528 M^{-1} for the binding constant. The absorbance and fluorescence experiments, thus, corroborate each other so far as the determination of binding constant is concerned and the mean value is calculated to be 531 M^{-1}. The relatively low value (normal values being in the range $10^3 - 10^4$ M^{-1})[11,12] of the binding constant for the present case is ascribed to the unfavourable situation because of the similar electrostatic character of the probe and the DNA phosphate backbone (both being negative). Using this binding constant (K) value, the free energy change for this DNA-probe binding is determined to be $\Delta G = -15.55$ kJ mol^{-1} exploiting the integrated form of vant Hoff's equation as given below.[25]

$$\Delta G = - RT \ln K$$

The negative value dictates a thermodynamically favourable

binding process. The order of the estimated binding constant indicates groove binding of the probe in the DNA environment, since for intercalative binding the binding constants are known to be much higher ($\sim 10^5$ M^{-1}).[35,36]
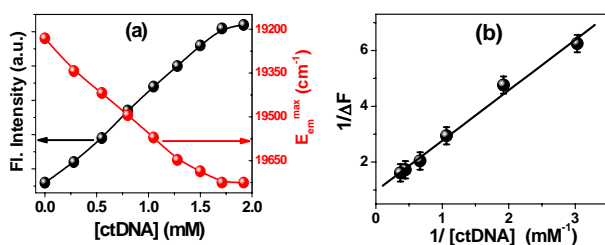
Fig. 3 (a) Plot of variation of the emission intensity (Black) and maximum of the fluorescence band (Red) of ANS as a function of ctDNA concentration. [ANS] = 10 μM. (b) Double reciprocal plot for the binding of ANS and ctDNA from fluorescence data.

Steady state fluorescence anisotropy study

Steady-state fluorescence anisotropy reflects the extent of restriction imposed by the microenvironment on the dynamic properties of the probe, and hence can be exploited in assessing the motional information of the probe in the microheterogeneous environments.[25,32] An increase in the rigidity in the local environment around a fluorophore causes an increase in the fluorescence anisotropy. The anisotropy value is very low in highly fluid solutions where the fluorophore can rotate almost freely. However, the anisotropy value goes up in confined media like protein, DNA, micelle, reverse micelle, cyclodextrin etc. where the rotation is restricted because of the interactions with the microheterogeneous environments.[10,32,37] Fig. 4 (a) illustrates the variation of the steady state fluorescence anisotropy of ANS with increasing ctDNA concentration. The plot reveals that with the gradual addition of ctDNA there is an increase in the fluorescence anisotropy (r) of ANS followed by attainment of a plateau with r ~0.11. The observation suggests imposition of a motional restriction on ANS within the ctDNA environment compared to that in the bulk aqueous medium. This is ascribed to a binding interaction between the probe and the DNA. It is important to note that the maximum fluorescence anisotropy value of DNA-bound probe is considerably less than the value expected for an intercalated probe.[10,12] This implies that ANS binds to ctDNA not through intercalative binding which generally yields higher anisotropy value (~0.20 or above) but through groove binding.

Determination of the polarity of the microenvironment

A good way to assess the location of the fluorophore in a microheterogeneous environment is to determine the polarity in the immediate vicinity around the probe.[12,32] The micropolarity in such an environment is often determined and expressed in equivalent $E_T(30)$ scale based on the transition energy for the solvatochromic intramolecular charge transfer absorption of the betaine dye, 2,6-diphenyl-4(2,4,6 triphenyl-1-pyridono)phenolate, as developed by Kosower and Reichardt[38,39] comparing the fluorescence behaviour of the probe in the microheterogeneous environment to that in a series of homogeneous solvent mixtures of varying composition with known $E_T(30)$ values. For the

present purpose, we have studied the fluorescence behavior of ANS in water-dioxane mixtures of varying composition.[40,41] The $E_T(30)$ values for different compositions of the dioxane-water mixtures are taken from the work of Kosower et al.[38] Justification of the choice of water/dioxane mixture over water/alcohol that is often used for such studies lies in the fact that the former covers a much wider range of polarity.[12]

Representative plot monitoring energy corresponding to the fluorescence maximum of the probe in the water-dioxane mixtures against $E_T(30)$ establishes a linear correlation between the two parameters (Fig. 4 (b)). Interpolating the values of the energies corresponding to the emission maxima of ANS in aqueous buffer and ctDNA environments on the calibration line, the micropolarity values around the probe in the two situations are determined. The values come out to be 62.4 ($\pm$ 0.2) kcal mol^{-1} and 57.6 ($\pm$ 0.2) kcal mol^{-1} for aqueous buffer milieu and ctDNA environment respectively. It is pertinent to mention here that, one should not be very serious about the absolute micropolarity values estimated for the aqueous buffer and DNA environment because of the possibilities of specific solvation in this solvent mixture as well as the gross approximation that the mixed solvents mimic the experimental environments. The study gives an indication that in ctDNA, ANS resides in an appreciably less polar environment compared to the bulk aqueous phase.
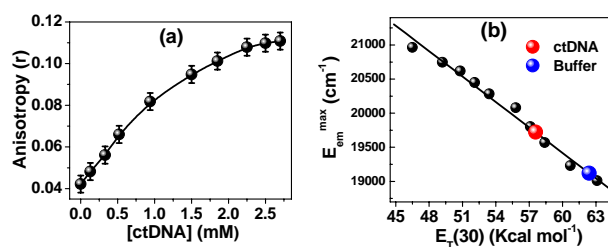
Fig. 4 (a) Variation of fluorescence anisotropy of ANS as a function of concentration of ctDNA. λ_{exc} = 370 nm, λ_{em} = 515 nm. [ANS] = 10 μM. (b) Variation of the energies corresponding to the maxima of the emission of ANS as a function of $E_T(30)$ in water-dioxane mixtures. The environments for the interpolated points are provided in the legends. [ctDNA] = 1.92 mM and [ANS] = 10 μM.

Comparative binding study with known DNA intercalator

To check if the binding of ANS with ctDNA is of groove or intercalative in nature, we have performed a comparative binding study with ethidium bromide (EtBr), a well known intercalative DNA binder.[42,43] Apart from the steady state fluorescence as represented in Fig. 5, fluorescence anisotropy has also been monitored for the purpose. Fig. 5 illustrates that with successive addition of EtBr to the ANS bound DNA, the emission intensity of EtBr (λ_{em}^{max} ~ 600 nm) increases drastically with imperceptible change in the ANS emission intensity (λ_{em}^{max} ~ 500 nm). The enormous increase in the emission intensity of the EtBr in DNA environment can be rationalized by considering the intercalative binding of EtBr with the ctDNA (already known). The inappreciable change in the emission intensity of DNA bound ANS with the addition of EtBr implies that the binding of EtBr through intercalation mode does not affect the binding of ANS with ctDNA. We have also performed the reverse

experiment, i.e., we have monitored the emission spectra of ctDNA bound EtBr in the presence of varying concentrations of ANS (Fig. S2 in the ESI). The experiment reveals that addition of ANS to the DNA bound EtBr does not bring any change in the

5 fluorescence intensity of EtBr while the emission intensity of ANS increases steadily, as expected because of the gradual addition of the fluorophore. This implies that the two probes, ANS and EtBr bind with ctDNA independently and binding of one probe with ctDNA does not affect the binding of the other.

10 Thus, the experiments confirm that ANS binds to ctDNA through groove binding mode since EtBr is known to bind to the ctDNA through intercalation.
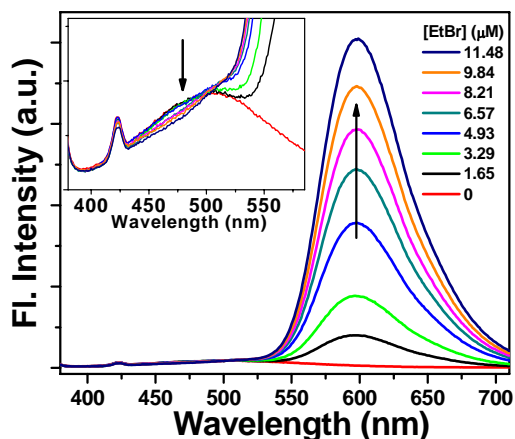
Fig. 5 Fluorescence spectra of ctDNA bound ANS with the addition of
15 **varying concentrations of EtBr. Concentrations of EtBr are labeled in the legends. Inset shows the same emission spectra in the lower wavelength range; λ_{exc} = 370 nm, [ctDNA] = 1.80 mM and [ANS] = 10 μM.**

As already discussed, gradual addition of ctDNA increases the
20 fluorescence anisotropy of ANS revealing binding between the host and the guest. Interestingly, with the addition of EtBr to the ANS bound DNA, there is hardly any meaningful change in the fluorescence anisotropy of ANS (from 0.11 to 0.10). This implies that the binding of EtBr with DNA does not affect the binding of
25 ANS with the host, suggesting that EtBr does not replace the other probe while binding with DNA. Fluorescence anisotropy of EtBr, however, increases from ~0.04 in buffered aqueous solution to ~0.22 in ctDNA environment, which is obviously due to the intercalation. Had the binding of ANS with ctDNA been
30 intercalative in nature, addition of EtBr to the ANS-DNA system would dislodge the bound ANS molecules from the DNA environment to the bulk aqueous medium. This should lead to a marked reduction in the fluorescence anisotropy of ANS. But the experimental observation goes against it and suggests that the
35 interaction between ANS and ctDNA is not intercalative, but groove binding in nature. The observed steady state anisotropy (r) values of ANS in aqueous buffer, 1.8 mM DNA and upon addition of 11.5 μM EtBr are collected in Table 1. Interestingly, the reverse experiment, i.e, addition of ANS to the DNA-bound
40 EtBr, does not make any change in the fluorescence anisotropy of the bound EtBr (r ~ 0.20) revealing that while binding with the ctDNA, ANS does not displace EtBr from its binding site. This corroborates the proposed binding mode of ANS with ctDNA.

45 A similar type of experiment was carried out by Jana et al. to elucidate the groove binding mode of 3-hydroxyflavone (3HF) in ctDNA.[12] They had shown that fluorescence anisotropy of ctDNA bound 3HF which binds with ctDNA through groove binding fashion, is not altered meaningfully by the addition of EtBr
50 whereas, anisotropy value of DNA bound quercetin, a well-known DNA intercalator[44] decreases remarkably and reaches the value that is observed in aqueous buffer by the gradual addition of EtBr.

Table 1. Steady state fluorescence anisotropy of ANS and EtBr in
55 different situations.

Sample	Monitoring wavelength (nm)	Fluorescence anisotropy (r)
ANS in buffer	515[a]	0.04
EtBr in buffer	620[b]	0.04
ANS in ctDNA	515[a]	0.11
ANS in ctDNA + EtBr	515[a]	0.10
ANS in ctDNA + EtBr	620[b]	0.22

[a]: λ_{exc} = 370 nm, [b]: λ_{exc} = 480 nm

Time resolved fluorescence decay study

Fluorescence lifetime measurement often serves as a sensitive
60 indicator of the local environment of a fluorophore and is responsive towards excited state processes.[7,11,33,45] In an attempt to follow a generalized picture of the interaction, we have opted for recording the fluorescence decays of ANS in the presence of varying concentrations of ctDNA. In aqueous buffer solution
65 ANS exhibits a single exponential fluorescence decay with a lifetime value of ~0.3 ns[18,23] but in ctDNA environment the decay becomes triexponential. Triexponential fluorescence decays of probes are quite common in microheterogeneous and/or biomacromolecular environments.[32] The multiexponential decay
70 of a polarity-sensitive probe molecule in microheterogeneous environments like the present one is reported to originate from the location of the different molecules of the same probe in regions differing in polarity and/or viscosity.[23,32] Typical decay profiles of ANS in the aforesaid environments are shown in Fig.
75 6, and the deconvoluted data are compiled in Table 2.
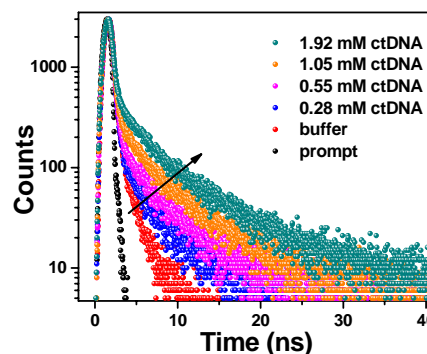
Fig. 6 Time resolved fluorescence decays of ANS in the absence and presence of ctDNA. The sharp black profile is the lamp profile. Concentrations of ctDNA are labeled in the legends. λ_{exc} = 370 nm,
80 **λ_{em} = 515 nm. [ANS] = 10 μM.**

Table 2. Time resolved fluorescence decay parameters of ANS in aqueous buffer and ctDNA environments

Solution	τ_1 (ns)	a_1	τ_2 (ns)	a_2	τ_3 (ns)	a_3	τ_{avg} (ns)	χ^2
Buffer	0.32	1.00					0.32	1.18
[ctDNA] mM								
0.28	0.27	0.975	1.53	0.020	6.13	0.005	0.33	1.09
0.55	0.30	0.968	1.69	0.023	6.31	0.009	0.39	1.12
1.05	0.30	0.957	2.02	0.030	7.16	0.013	0.44	1.20
1.50	0.31	0.948	2.55	0.038	8.62	0.014	0.51	1.13
1.92	0.31	0.940	2.83	0.040	9.05	0.020	0.58	1.08

A glance on Table 2 reflects that the shortest component (τ_1) of ANS remains almost same in DNA environment to that of aqueous buffer. So, this component (τ_1) may be assigned to the free (not bound to ctDNA) probe molecule. The other two components (τ_2 and τ_3) are ascribed to the DNA bound probe and they increase continuously with increasing ctDNA concentration. As a result, the average lifetime value (τ_{avg}) of ANS also increases significantly in DNA environment. An enhancement in the fluorescence lifetime of fluorophores in macromolecular environments indicates the binding interaction between them.[41,46] The data further suggest that with increasing ctDNA concentration more and more probe molecules bind to ctDNA resulting in a decrease in the amount of free probe (a_1) with concomitant increase in the amount of bound probe (a_2 and a_3).

Circular dichroism and helix melting study

That the mode of binding of ANS with ctDNA is not intercalative, has been established by adopting circular dichroism (CD) and DNA helix melting experiments, negative results of which eradicate the possibility of the binding mode to be intercalative. The secondary structure of DNA is known to be perturbed distinctly by the intercalation of small molecules leaving its signature through changes in the intrinsic CD spectra of the DNA.[10,47,48] Groove binding, however, does not put much impact on the CD profile.[7,11] Fig. 7 (a) represents the CD spectrum of ctDNA in HEPES buffer at pH 7, having a positive peak at ~275 nm and a negative peak at ~245 nm, characteristic of the right handed B form.[10,49] These bands are caused by the stacking interactions between the bases and the helical suprastructure of the polynucleotide that provides an asymmetric environment for the bases.[50] Gradual addition of ANS to the DNA solution does not reveal any significant change in the CD spectrum of DNA indicating that the binding of the probe with ctDNA does not disturb the stacking of the bases. This observation emphatically rules out the possibility of intercalation of ANS in the DNA helix, and thereby implies that the fluorophore binds to the host DNA through groove binding.

The groove binding of ANS with ctDNA has further been aptly corroborated from the DNA helix melting experiment. DNA melting is the process of separating the double helical DNA structure into two single strands.[51] With increasing temperature, the double helix structure of DNA is separated into single strands as heat spoils the hydrogen bonding and base stacking forces. The melting temperature (T_m) of DNA is defined as the temperature at which half of the double helical DNA strands are unfolded to single strands.[48] Helix melting of DNA is performed by measuring the absorbance at 260 nm as a function of temperature. The extinction coefficient of DNA bases at 260 nm in the double-

helical form is much less than in the single stranded form. Hence, the absorbance increases sharply as the helix melts and the DNA strands separate.[52] Stabilization of the helix because of the intercalation of probes results in an increase in the helix melting temperature of the DNA.[35,45] On the contrary, groove binding leads to an inappreciable change in the T_m value.[11,12] In the present study, experiment is carried out to monitor the change in T_m for ctDNA in the absence and presence of ANS to follow up the specific binding between them.
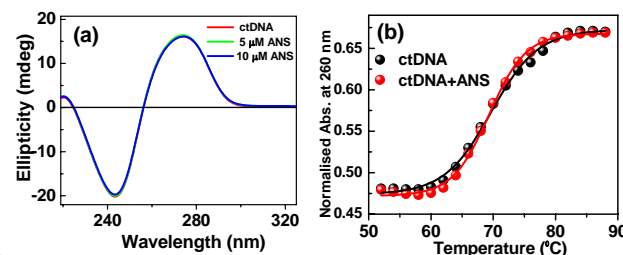
Fig. 7 (a) Representative CD spectra of ctDNA with varying concentrations of ANS. Concentrations of ANS are shown in the legends. [ctDNA] = 100 μM. (b) Thermal melting profiles of native ctDNA (30 μM) (black) and the same treated with 15 μM ANS (red).

We have determined T_m of the native ctDNA as well as the DNA in the presence of ANS separately (Fig. 7 (b)). The estimated melting temperatures come out to be 69.5 ($\pm$0.3) ^{0}C for both the free ctDNA and the probe bound DNA. The experiment reveals that upon binding with ANS, T_m of ctDNA does not change and hence, rules out the possibility of intercalation between the two interacting partners and stands in favour of groove binding.

Molecular docking analysis

Molecular docking simulation is frequently employed for finding the binding location of small molecules in the biomacromolecular structure including protein, DNA etc.[7,11,53,54] In order to get insight into ANS-ctDNA interaction and hence obtain the mode of binding of the probe with DNA, knowledge of proper binding location of the ANS into the ctDNA is important. So, we have performed the docking simulation study according to the protocol described in the Experimental Section. It is relevant to mention here that the outcome of the docking simulation depends on the crystallographic structure of DNA used.[55] For the present purpose, we have opted for B-DNA which is often used by different research groups to find the binding location of various molecular probes in DNA.[7,11] To achieve an unbiased result, the AutoDock based blind docking simulation has been employed. The strategy of AutoDock based blind docking comprises of an exploration over the entire macromolecule for possible binding sites and simultaneously optimizing the conformations of the macromolecule.[28,54] The docked conformation (Fig. 8) demonstrates that the ANS molecule exists in a crescent shape, which matches well with the natural curvature of the groove of the DNA. The estimated docking energy for the docked conformation is computed to be **-** 2.98 kcal mol^{-1} which is in agreement with the value of docking energy for the molecules which bind in a groove binding fashion with ctDNA.[11] Thus, the molecular docking study corroborates the experimental

observation of groove binding of ANS with ctDNA.
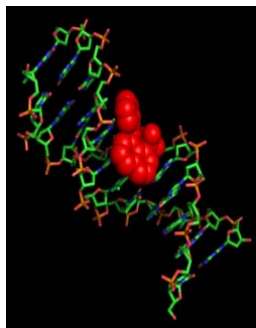
Fig. 8 Optimized docked pose of ANS (CPK model in red) with double stranded DNA.

The above sets of experiments together with molecular docking simulation have convincingly revealed that the biologically relevant anionic fluorophore, ANS binds with ctDNA through groove binding mode. Once the binding is established, we have made an endeavour to see if salts can be exploited to push the anionic probe more into the DNA environment with a long term goal of developing a strategy to push ionic drugs more into the target region to enhance the drug efficacy.

Effect of salt on ANS-ctDNA binding

Effect of ionic strength on the probe-DNA binding is usually employed to verify if there is significant electrostatic interaction between the probe and the DNA.[10,11,45] Increased ionic strength of the medium screens the electrostatic repulsion between the neighbouring phosphate groups, prompting the helix to shrink due to a decrease in the unwinding tendency caused by the electrostatic repulsion between the negatively charged phosphate groups.[10] Thus, an increase in the ionic strength leads to the weakening of binding interaction between the positively charged probe molecule and DNA due to the decreased electrostatic attraction between them and it has been observed for a number of positively charged probe molecules that bind with DNA.[10,45] Generally, binding interaction of a neutral probe with DNA is not affected appreciably by the ionic strength of the medium due to the aforementioned rationale.[11] Since the literature lacks reports on the effect of salts on the binding interaction of negatively charged probes with DNA, in the present work, we have made an endeavour to explore the salt effect on the ANS-DNA binding.

The emission behaviour of DNA bound ANS responses sharply to the addition of salts in the medium. In aqueous buffer medium ANS emission is quenched by the addition of NaCl (Fig. S3 in the ESI) due to chloride ion induced heavy atom/ion quenching[25], but in ctDNA environment we observe an opposite flurometric behaviour of ANS with the addition of NaCl. Fig. 9 (a) illustrates the variation in the fluorescence spectrum of ctDNA bound ANS in the presence of NaCl. The figure reveals that with increasing salt concentration the fluorescence intensity of DNA bound probe increases significantly with a substantial hypsochromic shift of 35 nm. The significant enhancement in the emission intensity of the probe in the DNA environment with increasing salt concentration can be rationalized by the enhanced

binding interaction between the ANS and ctDNA. The hypsochromic shift suggests that the probe which is already bound in the groove of DNA, experiences even lesser polar environment with the introduction of NaCl in the medium. Since the fluorescence of ANS is highly sensitive to the solvent polarity,[20] a minute change in the polarity and/or hydrophobicity of the microenvironment is reflected significantly in its emission characteristics.

The weak binding between ANS and DNA, as reflected from the low value of the binding constant, is ascribed to the electrostatic repulsion between the binding partners (both being negatively charged). The increased ionic strength of the medium screens this repulsion, and hence favours the binding process. We have adopted other steady state and time resolved fluorescence techniques to substantiate this rationale that probe-DNA binding is favoured by increased salt concentration.
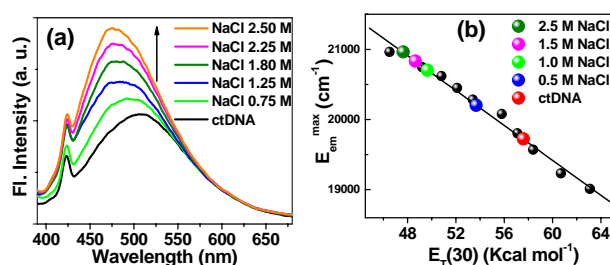
Fig. 9 (a) Representative emission profile of ctDNA bound ANS with increasing NaCl concentration. The concentrations of NaCl are labeled in the legends. λ_{exc} = 370 nm. [ctDNA] = 1.92 mM and [ANS] = 10 μM. (b) Variation of the energy corresponding to the maximum of the emission of ANS as a function of $E_T(30)$ in water-dioxane mixtures. The environments for the interpolated points are provided in the legends. [ctDNA] = 1.92 mM and [ANS] = 10 μM.

It is already mentioned that fluorescence anisotropy measurement provides information about the motional rigidity of a probe molecule around its microenvironment. To investigate the effect of salt on the dynamical property of the DNA bound ANS, we have exploited the steady state fluorescence anisotropy measurement. Fig. S4 (ESI) depicts the variation of the steady state fluorescence anisotropy of DNA-bound ANS with increasing NaCl concentration. Fig. S4 reveals that with increasing salt concentration fluorescence anisotropy value of DNA-bound ANS gradually increases before attainment of a saturation value of ~0.19. This observation supports the aforesaid rationale that introduction of salt favours the probe-DNA binding resulting in an enhanced motional restriction on ANS compared to that in the DNA environment in the absence of the added salt.

The increased ionic strength induced enhancement of the probe-DNA binding is expected to reduce the polarity of the microenvironment around the probe. To ascertain it, we have determined the $E_T(30)$ values of DNA-bound probe by interpolating the values of the energy corresponding to the emission maxima of ANS in DNA environment in the presence of NaCl on the previously obtained calibration line (Fig. 9 (b)). Fig. 9 (b) reveals that in the presence of NaCl, the micropolarity value around the DNA-bound probe decreases appreciably from that in the absence of the added salt. With increasing salt concentration the micropolarity value drops down steadily. Thus, the micropolarity analysis in the presence of added salt corroborates

the fluorometric results discussed above.

As fluorescence lifetime of a probe is very sensitive towards the local environment of the probe, we have performed the time resolved fluorescence decay measurements of DNA bound ANS in different salt concentrations. The time resolved decay profiles of DNA bound ANS in different salt concentrations are presented in Fig. 10 (a) and the analyzed data are collected in Table 3. The set of data in Table 3 reveals that with increasing NaCl concentration average lifetime (τ_{avg}) of DNA-bound probe increases significantly. Lifetime of ANS is known to be enhanced with decrease in the solvent polarity.[23] The change in the values of pre-exponential factors with increasing salt concentration is meaningful. A significant decrease in the relative amount of unbound probe molecules, reflected by the a_1 value (94% to 73%) and the increment in the average lifetime value (Table 3), in the presence of salt suggest that introduction of NaCl favours the binding process, substantiating the proposition made from the steady state flurometric studies.
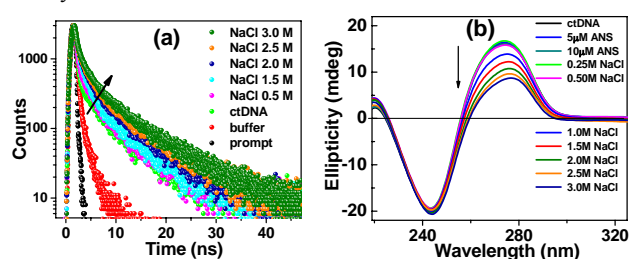
Fig. 10 (a) Time resolved fluorescence decay of ANS in buffer and DNA-bound ANS in presence of different salt concentrations. The sharp black profile is the lamp profile. Concentrations of NaCl are labeled in the legends. λexc = 370 nm. [ctDNA] = 1.92 mM and [ANS] = 10 μM. (b) Representative CD spectra of ANS bound ctDNA with varying concentrations of NaCl. Concentrations of NaCl are shown in the legends. [ctDNA] = 100 μM.

To decipher whether the salt itself brings any change in the secondary structure of ctDNA or not, circular dichroism (CD) spectral study of ctDNA in the absence and presence of different NaCl concentrations has been performed. Fig. 10 (b) represents the CD spectra of ANS-bound ctDNA with varying concentrations of NaCl. The Figure reveals that upto 0.5 M NaCl concentration, there is hardly any change in the CD spectrum of the probe bound DNA. On increasing the NaCl concentration further the CD spectrum changes appreciably, consistent with the previous literature report, and suggests that increased salt concentration results in a change in the secondary structure of DNA.[56] It is obvious from the Fig. 10 (b) that increasing salt concentration brings change mainly in the positive peak (275 nm) of the probe bound ctDNA whereas the negative peak (245 nm) remains almost unaffected by the salt. It is well known that the positive band of ctDNA at around 275 nm arises due to the base stacking and the negative band at around 245 nm is due to the helicity of the DNA structure.[11,13] Fig. 10 (b) suggests that with the introduction of NaCl, stacking interaction between the basepairs (A-T and G-C) of DNA changes while the helical structure of the double stranded DNA remains almost unchanged. Oslon and co-workers have shown that at high salt concentration DNA adopts a compact, highly bent and tightly intertwined structure.[57] Thus, it is highly probable that with increasing salt

concentration due to the change in DNA base stacking, the size of the DNA groove changes and the ANS molecule fits well within this resized groove. This tight fitting of the probe molecule within the DNA groove in the presence of NaCl together with the reduced electrostatic repulsion between the probe and DNA is ascribed to be responsible for the steady state and time resolved fluorescence behavior of the DNA-bound probe in the presence of added salt.

Table 3. Time resolved fluorescence decay parameters of DNA-bound ANS in different NaCl concentrations

Solution	τ_1 (ns)	a_1	τ_2 (ns)	a_2	τ_3 (ns)	a_3	τ_{avg} (ns)	χ^2
ctDNA	0.31	0.94	2.83	0.04	9.05	0.02	0.58	1.08
[NaCl] M								
0.25	0.36	0.87	1.93	0.107	7.74	0.023	0.70	1.14
0.5	0.33	0.89	2.41	0.085	8.88	0.025	0.72	1.11
1.0	0.32	0.86	2.31	0.104	8.90	0.036	0.84	1.09
1.5	0.39	0.76	1.99	0.18	8.92	0.06	1.19	1.16
2.0	0.42	0.76	2.10	0.19	8.96	0.05	1.16	1.08
2.5	0.38	0.77	2.18	0.175	9.31	0.055	1.19	1.13
3.0	0.43	0.73	2.35	0.20	9.64	0.07	1.46	1.11

Effect of other salts on the DNA-bound ANS

To confirm that ionic strength of the medium plays the key role in favouring the ANS-DNA binding in the presence of high salt concentration, we have further performed two sets of steady state fluorescence measurements; the first one with salts like sodium chloride (NaCl), sodium bromide (NaBr) and sodium iodide (NaI), all having the same valence nature (1:1) and the second one with sodium bromibe (NaBr), sodium sulfate (Na_2SO_4) and sodium phosphate (Na_3PO_4) having different valence nature (1:1, 1:2 and 1:3). In the first set of experiments we observe a similar extent of increment in the fluorescence intensity of the DNA bound probe in the presence of all the halide salts at the saturation level of interaction (Fig. 11 (a)). Corresponding emission spectra are provided in the ESI (Figs. S5 and S6). The hypsochromic shifts of the emission maxima of DNA bound ANS in the presence of salts is also found to be of the similar magnitude. It is, however, pertinent to mention here that at lower concentration, for both NaBr and NaI, we observe a small initial decrease in the emission intensity. Inset of Fig. 11 (a) shows the variation of the fluorescence intensity of DNA-bound ANS in the lower range of salt concentration. It clearly depicts that when the salt concentration is low the emission intensity decreases in the order $I^- > Br^- > Cl^-$ followed by a steady increase. This interesting observation can be explained by considering the relative quenching efficiency of the halide ions. Halides are well known quenchers following the efficiency of quenching in the order, $I^- > Br^- > Cl^-$.[25] The existing literature suggests that the DNA groove binder probes are partly accessible to the ionic quencher.[11,12] It appears that at low salt concentrations, the quenching of the accessible probe by the halide ions is more effective over the fluorescence enhancement due to the increase in the ionic strength.

In the second set of experiments plot of I/I_0 against the salt concentration (Fig. 11 (b)) shows that the increment in the emission intensity of the DNA-bound ANS follows the order $Na_3PO_4 > Na_2SO_4 > NaBr$. This implies that salt with trivalent

anion has the maximum effect followed gradually by the salts with bivalent and monovalent anions. Thus, the combined observations of these experiments confirm the role of ionic strength towards the binding of the probe with ctDNA.
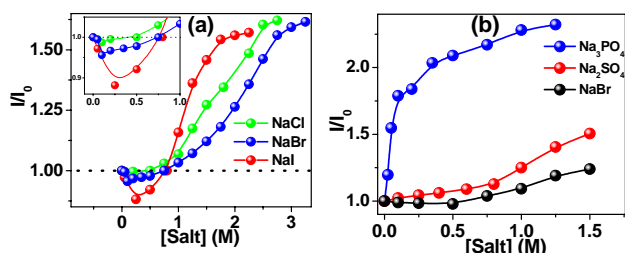
Fig. 11 (a) Variation of the relative fluorescence intensity (I/I₀) of ANS as a function of concentrations of the halide ion in 1.92 mM ctDNA solution. [ANS] = 10 μM. Inset shows the variation in lower concentration range. (b) Variation of the relative fluorescence intensity (I/I₀) of ANS as a function of concentrations of the monovalent, bivalent and trivalent anions in 1.92 mM ctDNA solution. [ANS] = 10 μM.

Conclusion

The present study reports the binding interaction of a biologically relevant fluorophore, ANS with calf thymus DNA. The steady state and time resolved fluorometric and other spectroscopic measurements unambiguously suggest the groove binding of the probe with the DNA. Molecular docking simulation corroborates the experimental results. The work further suggests that the binding of the probe with ctDNA is favoured by the increased ionic strength of the medium. This exertion is expected to provide a significant insight into the probe-DNA interaction. Further studies with other negatively charged dyes/drugs with DNA are encouraged for similar enhancement of drug-DNA binding interaction by the application of external salts.

Acknowledgements

Notes and references

[a]Department of Chemistry, Jadavpur University, Kolkata - 700 032, India
[b]Department of Chemistry, Indian Institute of Science Education and Research Bhopal,Bhauri, Bhopal 462066, Madhya Pradesh, India

*Corresponding author: Fax: 91-33-2414 6584
E-mail: nitin.chattopadhyay@yahoo.com

† Electronic Supplementary Information (ESI) available: Figures corresponding to the double reciprocal plot from absorption data, emission spectra for the competitive binding study with EtBr, emission spectra of ANS in the presence of different salt concentrations, variation of the fluorescence anisotropy (r) of ctDNA bound ANS against NaCl concentrations, and emission profile of ctDNA bound ANS with increasing concentration of both NaBr and NaI. See DOI: 10.1039/b000000x/

1   Y. Ma, G. Zhang and J. Pan, *J. Agric. Food Chem.*, 2012, **60**, 10867−10875.
2   Y. Fei, G. Lu and G. Fan, *Anal. Sci.*, 2009, **25**, 1333−1338.
3   X. L. Li, Y. J. Hu, H. Wang, B. Q. Yu and H. L. Yue, *Biomacromolecules*, 2012, **13**, 873−880.
4   L. Zhou, J. Yang, C. Estavillo, J. D. Stuart, J. B. Schenkman and J. F. Rusling, *J. Am. Chem. Soc.*, 2003, **125**, 1431−1436.
5   J. A. Lefstin and K. R. Yamamoto, *Nature*, 1998, **392**, 885−888.
6   V. Rajendiran, M. Murali, E. Suresh, M. Palaniandavar, V. S. Periasamy and M. A. Akbarsha, *Dalton Trans.*, 2008, **16**, 2157−2170.
7   D. Sahoo, P. Bhattacharya and S. Chakravorti, *J. Phys. Chem. B*, 2010, **114**, 2044−2050.
8   D. Bhowmik, M. Hossain, F. Buzzetti, R. D'Auria, P. Lombardi and G. S. Kumar, *J. Phys. Chem. B*, 2012, **116**, 2314−2324.
9   W. Saenger, *Principles of Nucleic Acid Structure*; Springer-Verlag: New York, 1983.
10 D. Sarkar, P. Das, S. Basak and N. Chattopadhyay, *J. Phys. Chem. B*, 2008, **112**, 9243−9249.
11 S. S. Mati, S. S. Roy, S. Chall, S. Bhattacharya and S. C. Bhattacharya, *J. Phys. Chem. B*, 2013, **117**, 14655−14665.
12 B. Jana, S. Senapati, D. Ghosh, D. Bose and N. Chattopadhyay, *J. Phys. Chem. B*, 2012, **116**, 639−645.
13 S. Bhattacharya, G. Mandal and T. Ganguly, *J. Photochem. Photobiol. B: Biol.*, 2010, **101**, 89−96.
14 Y. Li, R. Geyer and D. Sen, *Biochemistry*, 1996, **35**, 6911−6922.
15 E. B. Abuin, E. A. Lissi, E. Alexisaspe, F. D. Gonzalez and J. M. Varas, *J. Colloid Interface Sci.*, 1997, **186**, 332−338.
16 L. Brand and J. R. Gohlke, *Annu. Rev. Biochem.*, 1972, **41**, 843−868.
17 J. Sujatha and A. K. Mishra, *J. Photochem. Photobiol. A*, 1997, **104**, 173−178.
18 A. C. Kumar, H. Erothu, H. B. Bohidar and A. K. Mishra, *J. Phys. Chem. B*, 2011, **115**, 433−439.
19 K. Sahu, S. K. Mondal, S. Ghosh, D. Roy and K. Bhattacharyya, *J. Chem. Phys.*, 2006, **124**, 124909/1−7.
20 M. Mohapatra and A. K. Mishra, *Langmuir*, 2013, **29**, 11396−11404.
21 M. E. Mohanty and A. K. Mishra, *J. Polym. Res.*, 2013, **20**, 185/1−8.
22 E. Schonbrunn, S. Eschenburg, K. Luger, W. Kabsch and N. Amrhein, *Proc. Natl. Acad. Sci. U.S.A.*, 2000, **97**, 6345−6349.
23 D. Sarkar, D. Ghosh, P. Das and N. Chattopadhyay, *J. Phys. Chem. B*, 2010, **114**, 12541−12548.
24 I. Saha and G. S. Kumar, *J. Fluoresc.*, 2011, **21**, 247−255.
25 J. R. Lakowicz, *Principles of Fluorescence Spectroscopy*, 3rd Edn., Springer, New York, 2006.
26 H. R. Drew, R. M. Wing, T. Takano, C. Broka, S. Tanaka, K. Itakura and R. E. Dickerson, *Proc. Natl. Acad. Sci. U.S.A.*, 1981, **78**, 2179−2183.
27 M. J. Frisch, G. W. Trucks, H. B. Schlegel, G. E. Scuseria, M. A. Robb, R. J. Cheeseman, J. A. Jr. Montgomery, T. Vreven, K. N. Kudin and J. C. Burant, et al., *Gaussian 03*, revision E.01; Gaussian, Inc.: Wallingford, CT, 2004.
28 G. M. Morris, D. S. Goodsell, R. S. Halliday, R. Huey, W. E. Hart, R. K. Belew and A. J. Olson, *J. Comput. Chem.*, 1998, **19**, 1639−1662.
29 W. L. De Lano, *The PyMOL Molecular Graphics System,* De Lano Scientific: San Carlos, CA, 2004.
30 S. Ghosh, S. Chattoraj and K. Bhattacharyya, *J. Phys. Chem. B*, 2014, **118**, 2949−2956.
31 H. A. Benesi and J. H. Hildebrand, *J. Am. Chem. Soc.*, 1949, **71**, 2703−2707.
32 A. Chakrabarty, A. Mallick, B. Haldar, P. Das and N. Chattopadhyay, *Biomacromolecules*, 2007, **8**, 920-927.
33 A. Mallick, B. Haldar and N. Chattopadhyay, *J. Phys. Chem. B*, 2005, **109**, 14683-14690.
34 A. Mallick and N. Chattopadhyay, *Photochem. Photobiol.*, 2005, **81**, 419-424.
35 S. Das and G. S. Kumar, *J. Mol. Struct.*, 2008, **872**, 56−63.
36 I. Saha, M. Hossain and G. S. Kumar, *J. Phys. Chem. B*, 2010, **114**, 15278-15287.
37 P. Das, A. Chakrabarty, B. Haldar, A. Mallick and N. Chattopadhyay, *J. Phys. Chem. B*, 2007, **111**, 7401-7408.

38 E. M. Kosower, H. Dodiuk, K. Tanizawa, M. Ottolenghi and N. Orbach, *J. Am. Chem. Soc.*, 1975, **97**, 2167-2178.

39 C. Reichardt, *Molecular Interactions*; Ratajazak, H.; Orville Thomas, W. J. Eds. Wiley: New York, 1982, **3**.

5 40 D. Bose, D. Ghosh, P. Das, A. Girigoswami, D. Sarkar and N. Chattopadhyay, *Chem. Phys. Lipids*, 2010, **163**, 94-101.

41 A. Mahata, D. Sarkar, D. Bose, D. Ghosh, A. Girigoswami, P. Das, and N. Chattopadhyay, *J. Phys. Chem. B*, 2009, **113**, 7517-7526.

42 L. S. Lerman, *J. Mol. Biol.*, 1961, **3**, 18-30.

10 43 L. S. Lerman, *Proc. Natl. Acad. Sci. U.S.A.*, 1963, **49**, 94-102.

44 Z. Zhu, C. Li and N. Q. Li, *Microchem. J.*, 2002, **71**, 57–63.

45 B. K. Paul and N. Guchhait, *J. Phys. Chem. B*, 2011, **115**, 11938−11949.

46 D. Sarkar, A. Mahata, P. Das, A. Girigoswami, D. Ghosh and N. 15 Chattopadhyay, *J. Photochem. Photobiol. B: Biol.*, 2009, **96**, 136−143.

47 S. S. Jain, M. Polak and N. V. Hud, *Nucleic Acids Res.*, 2003, **31**, 4608-4615.

48 J. L. Mergny, G. Duval-Valentin, C. H. Nguyen, L. Perrouault, B. 20 Faucon, M. Rougée, T. Montenay-Garestier, E. Bisagni and C. Hélène, *Science*, 1992, **256**, 1681-1684.

49 K. van Holde, W. C. Johnson and P. S. Ho, *Principles of Physical Biochemistry*; Prentice Hall: New York, 1998.

50 Y. F. Long, Q. G. Liao, C. Z. Huang, J. Ling and Y. F. Li, *J. Phys.* 25 *Chem. B*, 2008, **112**, 1783-1788.

51 S. S. Wijeratne, J. M. Patel and C. H. Kiang, *Rev. Plasmonics*, 2012, **2010**, 269−282.

52 P. Nagababu, J. N. L. Latha, Y. Prashanthi and S. Satyanarayana, *J. Chem. Pharm. Res.*, 2009, **1**, 238−249.

30 53 B. K. Paul, D. Ray and N. Guchhait, *Phys. Chem. Chem. Phys.*, 2012, **14**, 8892–8902.

54 S. J. Campbell, N. D. Gold, R. M. Jackson and D. R. Westhead, *Curr. Opin. Struct. Biol.*, 2003, **13**, 389–395.

55 C. G. Ricci and P. A. Netz, *J. Chem. Inf. Model.*, 2009, **49**, 1925– 35 1935.

56 D. S. Studdert, M. Patroni and R. C. Davis, *Biopolymers*, 1972, **11**, 761–779.

57 T. Schlick, L. Bin and K. Oslon, *Biophys. J.*, 1994, **67**, 2146–2166.

TABLE OF CONTENTS

Groove binding of ANS with ctDNA
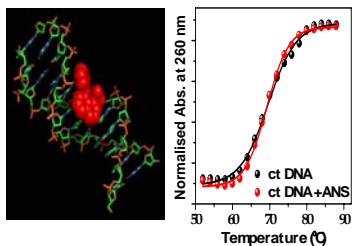
5 Binding mode of biologically relevant anionic probe, ANS, with ctDNA is divulged from spectroscopic and molecular docking studies.

10